Nonlinear dynamics of semiconductor lasers under repetitive optical pulse injection

Fan-Yi Lin, Shiou-Yuan Tu, Chien-Chih Huang, and Shu-Ming Chang

Abstract—**Nonlinear dynamics of semiconductor lasers under repetitive optical pulse injection are studied numerically. Different dynamical states, including pulsation and oscillation states, are found by varying the intensity and the repetition rate of the injection pulses. The laser is found to enter the chaotic pulsation (CP) states and chaotic oscillation (CO) states through individual period-doubling routes. Mapping and corresponding Lyapunov exponents of these dynamical states are plotted and examined in the parameter space. Moreover, the bandwidths of the chaos states found are investigated, where the bandwidths of the CP states observed at the strong injection regime are two to four times broader than the bandwidths of the CO states found at the weak injection regime. In this paper, frequency-locked states with different winding numbers, the ratio of the oscillation frequency and the repetition frequency of the injection pulses, are also studied. Both the cases for repetition frequency above and below the relaxation oscillation frequency are examined. The winding numbers of the frequency-locked states reveal a Devil's staircase structure, where a Farey tree showing the relations between the neighboring states is constructed.**

I. INTRODUCTION

NONLINEAR dynamical characteristics of semiconductor lasers have been studied intensively in recent years. Diverse dynamical states found have been proposed to be utilized in various applications such as radar [1], lidar [2], [3], radio-over-fiber communications [4], and chaotic communications [5], [6], [7], [8]. For an optically injected laser with a master-slave configuration, bandwidth enhancement [9], [10], linewidth reduction [11], [12], and noise suppression [13] phenomena have been observed. By controlling the injection strength and the frequency detuning between the master and the slave lasers, induced periodic oscillations and chaotic oscillations have been obtained [14], [15]. Both period-doubling [16] and break-up of two tori [17] routes to chaos have been reported. However, although many efforts have been made to understand the characteristics of an optically injected semiconductor laser [18], researches are limited to the condition where the laser is injected with an optical signal of constant intensity. Few studies have been done on the nonlinear dynamics of a semiconductor laser subjects to a non-constant optical injection.

Non-constant optical injection is important when a transmitter-receiver or a cascaded laser system is considered,

Fan-Yi Lin and Shiou-Yuan Tu are with the Institute of Photonics Technologies, Department of Electrical Engineering, National Tsing Hua University, Hsinchu 300, Taiwan e-mail: fylin@ee.nthu.edu.tw

Chien-Chih Huang is with the Department of Mathematics, National Tsing Hua University, Hsinchu 300, Taiwan

Shu-Ming Chang is with the Department of Applied Mathematics, National Chiao Tung University, Hsinchu 300, Taiwan e-mail: sm-chang@math.nctu.edu.tw

in which the dynamical output of a transmitter laser can optically inject into a receiver laser inevitably or even intentionally. With a chaotic optical injection, high-frequency broad-band signal generation has been demonstrated [19]. By injecting optical pulses at a subharmonic of the cavity round-trip frequency, a long cavity multisection semiconductor laser oscillating at its resonant frequency has been observed [20]. Repetitive pulses with twice the period have been observed in a Fabry-Perot laser subject to optical pulse injection [21]. Mode locking in broad-area semiconductor lasers by injecting optical pulses repeated at subharmonics of the lateral mode separation has been demonstrated [22]. In this paper, we study the complex dynamics of a semiconductor laser induced by optical pulses. By injecting a laser with a train of repetitive pulses, various dynamical states are shown and routes to chaos are identified. The dynamical mapping of the states is plotted and the bandwidths of the chaos states are investigated. Moreover, frequency locking phenomena driven by the pulse injection are also examined.

II. SIMULATION MODEL

The schematic setup of an optical pulse injected semiconductor laser is shown in Fig. 1. The laser is injected by a train of optical pulses, where the repetition rate and the intensity of the pulse train are varied as the controllable parameters. The dynamics of the injected laser are simulated using the model described in [23] with the following normalized dimensionless rate equations:

$$\frac{da}{dt} = \frac{1}{2}[\frac{\gamma_c \gamma_n}{\gamma_s \tilde{J}}\tilde{n} - \gamma_p(2a + a^2)](1 + a)$$
$$+ \xi_i(t)\gamma_c \cos(\Omega t + \phi),$$
$$\frac{d\phi}{dt} = -\frac{b}{2}[\frac{\gamma_c \gamma_n}{\gamma_s \tilde{J}}\tilde{n} - \gamma_p(2a + a^2)]$$
$$- \frac{\xi_i(t)\gamma_c}{1 + a}\sin(\Omega t + \phi),$$
$$\frac{d\tilde{n}}{dt} = -\gamma_s \tilde{n} - \gamma_n(1 + a)^2 \tilde{n} - \gamma_s \tilde{J}(2a + a^2)$$
$$+ \frac{\gamma_s \gamma_p}{\gamma_c}\tilde{J}(2a + a^2)(1 + a)^2,$$

where, a is the normalized field, ϕ is the optical phase, $\tilde{n}$ is the normalized carrier density, b is the linewidth enhancement factor, γ_c is the cavity decay rate, γ_s is the spontaneous carrier decay rate, γ_n is the differential carrier relaxation rate, γ_p is the nonlinear carrier relaxation rate, and $\tilde{J}$ is the normalized dimensionless injection current parameter. The dimensionless injection parameter $\xi_i(t) = \eta|A_i(t)|/(\gamma_c|A_0|)$

is the normalized strength of the injection field received by the injected laser where η is the coupling rate, $A_i(t)$ is the complex amplitude of the injection field, and A_0 is the complex field amplitude of the injected laser at free-running. The frequency detuning Ω is the frequency difference between the pulsed laser and the injected laser at free-running.
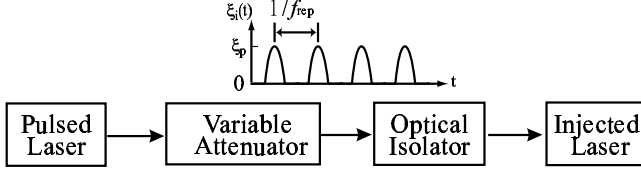

Fig. 1. Schematic setup of a semiconductor laser under repetitive optical pulse injection. The variable attenuator is used to adjust the injection strength and the optical isolator is used to prevent the unwanted feedback.
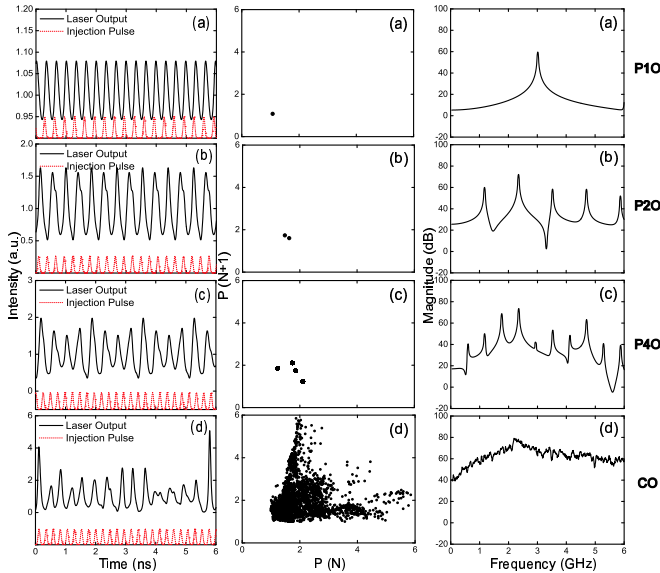

Fig. 2. Time series, phase portraits, and power spectra of different oscillation states with (ξ_p, f_{rep}) = (a) P1O (0.01, 3.0), (b) P2O (0.02, 3.5), (c) P4O (0.03, 3.8), and (d) CO (0.04, 4.0). The dashed curves in the time series are the corresponding waveforms of the injected pulses showing the timing of injection, which are scaled for clarity.

For the repetitive injection pulse train, a Gaussian shape of $\xi_i(t)$ with a peak injection strength ξ_p, a repetition frequency f_{rep}, and a pulsewidth of 75 ps are considered. Following experimentally measured intrinsic dynamical parameters of a high-speed semiconductor laser [24] are used in the simulation: $\gamma_c = 2.4 \times 10^{11}s^{-1}$, $\gamma_s = 1.458 \times 10^{9}s^{-1}$, $\gamma_n = 3\tilde{J} \times 10^{9}s^{-1}$, $\gamma_p = 3.6\tilde{J} \times 10^{9}s^{-1}$, $b = 4$, while zero detuning ($\Omega = 0$) is assumed. The lasers are biased at a value of $\tilde{J} = 1/3$ and the relaxation oscillation frequency ($f_r = (\gamma_c\gamma_n + \gamma_s\gamma_p)^{1/2}/2\pi$) of the laser is about 2.5 GHz with the aforementioned parameters. Second-order Runge-Kutta method with a sampling time of 2.38 ps is used to solve the coupled rate equations.

III. RESULTS

A. Nonlinear dynamical states

When a laser is injected by a single optical pulse, induced oscillations in the laser output field are expected and the laser tends to relax back to its free-running state gradually if no successive pulse is further injected. However, if a train of optical pulses are injected into the laser with the time separation between each successive pulse being shorter than the relaxation time of the laser, the relaxed oscillation will be interrupted while the injected pulses perturb the optical field and phase abruptly. Hence, the nonlinear dynamics of an optical pulse injection system is expected to be strongly influenced by the intensity and the repetition frequency of the injected pulses.
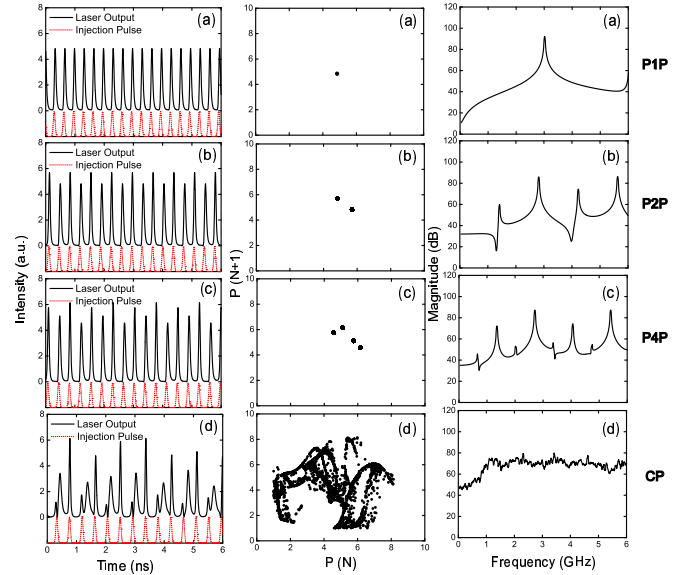

Fig. 3. Time series, phase portraits, and power spectra of different pulsation states with (ξ_p, f_{rep}) = (a) P1P (0.13, 3.0), (b) P2P (0.15, 2.8), (c) P4P (0.16, 2.7), and (d) CP (0.17, 2.3). The dashed curves in the time series are the corresponding waveforms of the injected pulses showing the timing of injection, which are scaled for clarity.

Figure 2 shows the time series, phase portraits, and power spectra of the dynamical states found in the optical pulse injection system. The dashed curves in the time series are the corresponding waveforms of the injected pulses showing the timing of injection, which are scaled for clarity. The phase diagrams in the second column are constructed by plotting the peak values of intensities of the N-th peak (P(N)) to the (N+1)-th peak (P(N+1)) taken from the time series shown in the first column, which reveals the complex attractors of the states as time evolves. As can be seen in Fig. 2(a), for peak injection strength ξ_p and repetition frequency f_{rep} (in GHz) of $(\xi_p, f_{rep}) = (0.01, 3.0)$, a period-1 oscillation (P1O) state is found and a single dot is shown in the phase diagram. The laser oscillates at the same frequency (3 GHz) as the repetition frequency f_{rep} of the injected pulses. Compared to the oscillation frequencies of the similar P1O states found in a laser with constant CW injection that increases along as the injection strength increases, the oscillation frequencies of the P1O states found in our study are not affected by the injection

strength (before the laser enters into another state) but are locked to the repetition frequency of the pulse injected. When ξ_p and f_{rep} are both increased to $(\xi_p, f_{rep}) = (0.02, 3.5)$, as shown in Fig. 2(b), a period-2 oscillation (P2O) state is obtained and two dots are observed in the phase diagram. As can be seen, the laser now oscillates at about 2.33 GHz and an envelope in the time series with a subharmonic frequency of the oscillation frequency is found. Further increases in ξ_p and f_{rep} drive the laser into a period-4 oscillation (P4O) and chaotic oscillation (CO) states as shown in Figs. 2(c) and (d), respectively. Clearly, the laser follows a period-doubling route into chaos when the parameters of the injected pulses are varied.

While these oscillation states have also been observed in an injected laser subject to constant injection, pulsation states are also found in this pulse injected laser system. Figure 3 shows the time series, phase portraits, and power spectra of the pulsation states observed. The dashed curves in the time series are the corresponding waveforms of the injected pulses showing the timing of injection, which are scaled for clarity. With $(\xi_p, f_{rep}) = (0.13, 3.0)$, Fig. 3(a) shows the regular pulsing (P1P) state, in which the laser pulses repetitively at the frequency of f_{rep}. When f_{rep} decreases, a period-2 pulsation state (P2P) that has a subharmonic envelope in the time series is observed. Further reducing f_{rep} drives the laser pulses with the fourth harmonic frequency (P4P), and goes into chaotic pulsing state (CP) eventually through a similar period-doubling route as in the oscillation counterpart. These pulsation states are clearly distinguishable from the oscillation states such that the peak intensity of the pulsation states is higher and it drops to zero between each subsequent pulse. Note that with repetitive pulse injection, these states shown in Figs. 2 and 3 are not transient states but states with dynamical stability. Moreover, while all the spectral harmonics of the injected pulses inevitably affect the laser dynamics implicitly, the lower harmonics, especially the 1st harmonic frequency f_{rep}, predominate due to both their larger amplitudes and higher responses near the relaxation oscillation frequency of the laser.

To show the regions of different dynamical states (as those shown in Figs. 2 and 3) occupied in the parameter space, a mapping is plotted in Fig. 4(a). As can be seen, regions of different dynamical states are identified, while the period-doubling routes for the oscillation states and the pulsation states can be traced. As shown in the mapping, the oscillation states are generally found in the weak injection regime ($\xi_p < 0.1$) while the pulsation states are observed in the stronger injection regime ($\xi_p > 0.1$). As ξ_p increases, the laser output gradually transforms from oscillations into pulsations as the duty-cycle of the waveforms decrease. Note that a belt of complex dynamical states, namely the CO and the CP states, is found stretching from the regime of weak injection-high repetition rate (> 2.5 GHz) to the regime of strong injection-low repetition rate (< 2.5 GHz). Within the belt, the CO states gradually transform into the CP states as ξ_p increases. To quantify the complexity of these states, Fig. 4(b) plots the corresponding largest Lyapunov exponents. As can be seen, while the P1P states in the upper right corner have
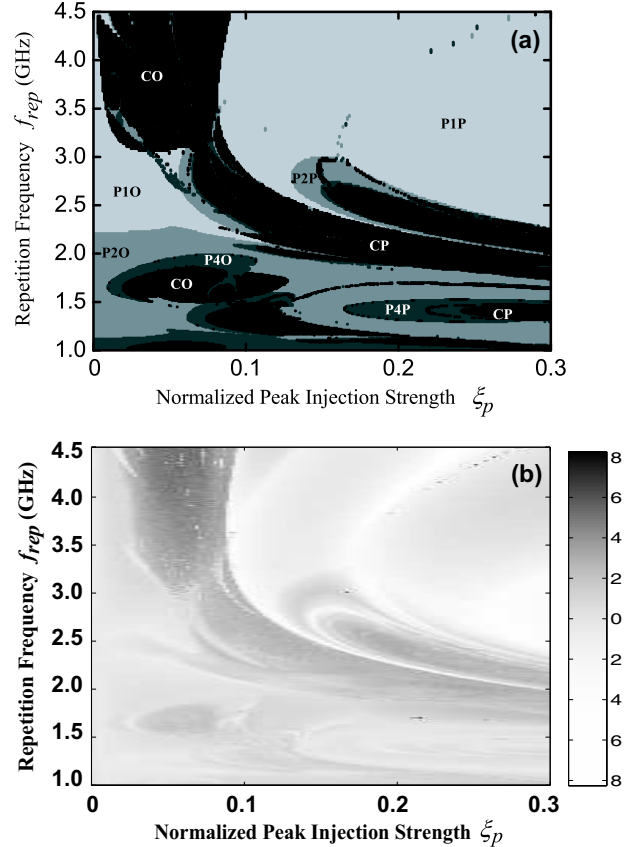

Fig. 4. (a) Mapping and corresponding (b) Lyapunov exponents of the dynamical states in the parameter space. P1O: period-1 oscillation; P2O: period-2 oscillation; P4O: period-4 oscillation; CO: chaotic oscillation; P1P: regular pulsation; P2P: period-2 pulsation; P4P: period-4 pulsation; and CP: chaotic pulsation.

negative Lyapunov exponents, positive Lyapunov exponents are found for those states showing complex dynamics seen in Fig. 4(a). Within the belt, CO states found in the upper left corner have the largest Lyapunov exponents and thus reveal their high complexities. While the behaviors and nonlinear dynamical characteristics for different frequency detunings are generally different, for simplicity, we only show the dynamical states and the corresponding mapping obtained with a single frequency detuning $\Omega = 0$ and emphasize the effects of the repetition frequency and the injection strength of the injected pulses. In all aspects, however, frequency detuning is no doubt a significant parameter affecting the laser dynamics as one would expect as in a CW optical injection case. Detailed investigation on the effect of frequency detuning in a pulse injected laser will be reported separately.

While some applications utilize chaos states to take the advantages of their high complexities for security reasons [5], [6], other applications, such as CLIDAR [2] and CRADAR [1], solely demand large-amplitude random signals with continuous broad bandwidths. As can be seen in Figs. 2(d) and 3(d), chaotic signals with continuous broad bandwidths can be induced through optical pulse injection. The bandwidths of those chaos states, CO and CP, found in the dynamical
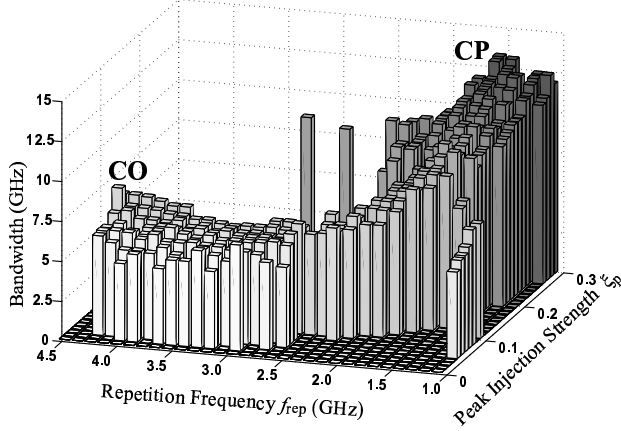
Fig. 5. Bandwidths of the chaotic oscillation (CO) states and chaotic pulsation (CP) states.
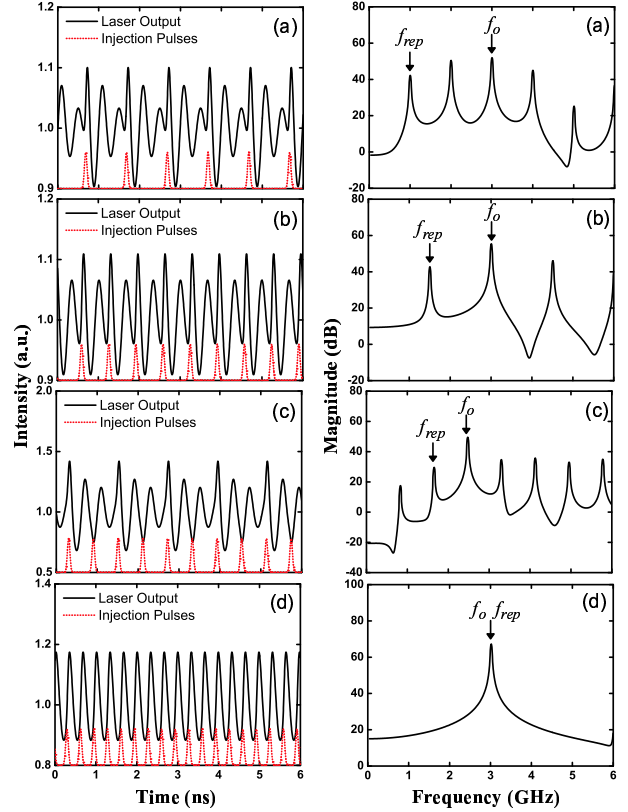

Fig. 6. Time series and power spectra of the frequency-locked states with $\xi_p = 0.02$ and $f_{rep} =$ (a) 1 ($\rho = 3/1$), (b) 1.5 ($\rho = 2/1$), (c) 1.65 ($\rho = 3/2$), and (d) 3 GHz ($\rho = 1/1$), respectively. The dashed curves in the time series are the injection pulse train, which are scaled for clarity. The arrows in the power spectra indicate f_{rep}.

mapping are therefore examined. Figure 5 plots the bandwidths of the chaos states with different parameters of the injected pulses. Due to the noise-like nature of the chaos states, the bandwidth of a chaos state is defined as the frequency span such that 80% of the energy is contained within. As can be seen, the bandwidths of the chaos states increase as ξ_p increases. Compared with the CO states found at the weak injection regime, the bandwidths of the CP states observed at the strong injection regime have bandwidths that are two to four times broader. For $\xi_p = 0.3$, chaos states with bandwidths as high as 14 GHz can be obtained for the laser with $f_r = 2.5$ GHz.

B. Frequency locking phenomenon

Frequency locking can occur in nonlinear systems when a driving frequency is an integer multiple or submultiple of an intrinsic frequency. If the two competing frequencies are however incommensurate, quasiperiodic oscillations are present instead. For semiconductor lasers, frequency locking has been found in direct current modulated self-pulsing lasers [25] and external-cavity lasers [26], where the pulsation frequency and the resonant frequency of the external cavity are locked to a rf modulation frequency, respectively. By feeding back the laser output optoelectronically through the bias current, harmonic frequency locking phenomenon has also been observed [27].

While these previous studies all involve electronic modulations through the bias current of the lasers, the phenomenon of semiconductor lasers subject to optical pulse injection is explored the first time. Instead of locking a laser by sending a modulation frequency through the bias current electronically, frequency locking driven by injecting optical pulses is investigated. Without the limitation of electronic bandwidths, the region that the repetition frequency of the optical pulses below and exceed the relaxation oscillation frequency of the laser are both examined.

Figure 6 shows the time series and power spectra of the output of a semiconductor laser under repetitive optical pulse injection with the normalized peak injection strength ξ_p fixed

at 0.02 while the repetition frequency f_{rep} is varied from 1 to 3 GHz. Here f_o is determined both from the highest peak seen in the power spectrum and the oscillation time interval shown in the time series. For $f_{rep} = 1$ GHz as shown in Fig. 6(a), a frequency-locked oscillation with an oscillation frequency $f_o = 3$ GHz is observed. The winding number, defined as $\rho = f_o/f_{rep}$, has a rational value $p/q = 3/1$ meaning that the oscillation frequency (f_o) of the laser output locks to the third-harmonic of the repetition frequency ($3f_{rep}$) of the injected pulses. Respectively, p and q are integer numbers defining the order of harmonics of f_o and f_{rep} in terms of the integer multiples of the lowest frequency peak seen in the spectrum. By increasing f_{rep} to 1.5 and 1.65 GHz, frequency-locked oscillations with $\rho = 2/1$ and $3/2$ as shown in Figs. 6(b) and (c) are found. Further increasing f_{rep} to 3 GHz drives the laser into a period-1 oscillation state with $\rho = 1/1$ as shown in Fig. 6(d), in which the laser oscillates sinusoidally at f_{rep}. In this system, the repetition frequency is interacting and competing with the intrinsic relaxation oscillation frequency of the laser through the injected pulses. While the repetition frequency is a hard fixed value determined by the external injected pulses, the oscillation frequency of the laser is rather flexible. In a frequency locked condition, f_o can be either pulled or pushed away from the intrinsic relaxation oscillation frequency f_r of the free-running condition and maintains
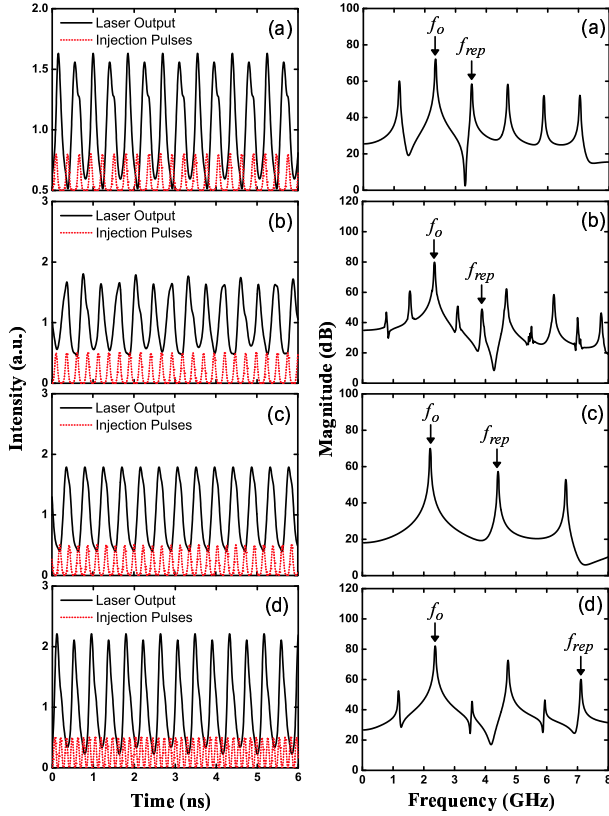
Fig. 7. Time series and power spectra of the frequency-locked states with $\xi_p = 0.02$ and $f_{rep} =$ (a) 3.5 ($\rho = 2/3$), (b) 3.85 ($\rho = 3/5$), (c) 4.4 ($\rho = 1/2$), and (d) 7 GHz ($\rho = 1/3$), respectively. The dashed curves in the time series are the injection pulse train, which are scaled for clarity. The arrows in the power spectra indicate f_{rep}.

injected laser gradually becomes similar to a laser injected by high-frequency sinusoidal excitation. However, unlike small-signal modulations, the laser is in fact under a high-frequency modulation with a very large modulation depth, where the injection strength goes to almost zero between each successive pulse. To the best of our knowledge, this is the first study on frequency locking of semiconductor lasers with an external frequency exceeding the relaxation oscillation frequency. For these states, the laser output still oscillates around the relaxation oscillation frequency as that is in the low-repetition frequency cases shown in Fig. 6.
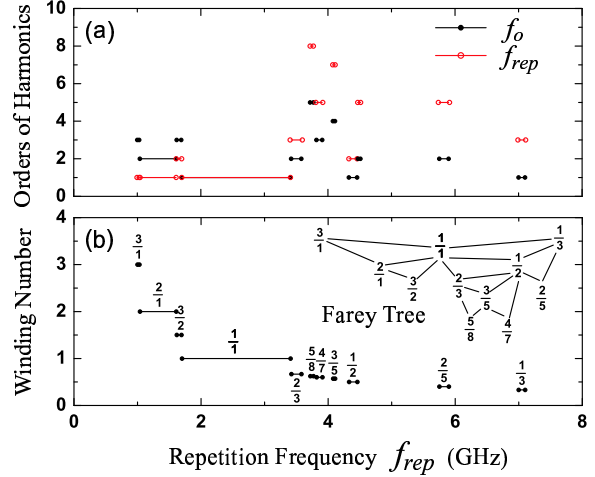

Fig. 8. (a) Order of harmonics of f_{rep} (opened circle) and f_o (closed circle) and (b) winding numbers of the frequency-locked oscillation states found for different repetition frequencies, respectively, where the widths of the intervals represent the ranges of locking. The upper right corner of 8(b) shows the Farey tree constructed by the Farey fractions of the corresponding frequency-locked states observed.
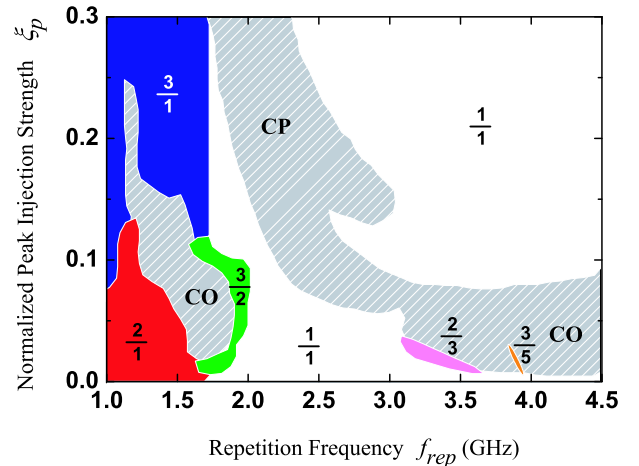
commensurate to f_{rep} with a Farey fraction within a certain tuning range. Nonetheless, the laser shows the tendency to oscillate in a frequency near f_r (2.5 GHz in our case). As a result, for different f_{rep}, frequency-locked states of different winding numbers are observed where f_o tends to lock to the harmonics of f_{rep} while staying close to f_r at the same time.

Unlike the modulation frequency of a current-modulated semiconductor laser which is inevitably limited by the modulation bandwidth, the repetition frequency of the injected optical pulses can exceed the relaxation oscillation frequency of the laser without the constraint. Figure 7 shows the time series and power spectra of the frequency-locked oscillations found for f_{rep} varies from 3 to 7 GHz. For $f_{rep} = 3.5$ GHz, a frequency-locked state with $\rho = 2/3$ is observed. Frequency-locked states of $\rho = 3/5$, 1/2, and 2/6 (1/3) are also shown in Figs. 7(b), (c), and (d), respectively, where f_o is the subharmonic of f_{rep}. As can be seen in Fig. 7(c), a period-1 oscillation is observed which f_o is exactly one-half of f_{rep} for the injected pulses. For f_{rep} as high as 7 GHz, frequency-locked state can still be found which the oscillation frequency is locked to the repetition frequency with $\rho = 2/6 \ (= 1/3)$. Different from a pure $\rho = 1/3$ state, the $\rho = 2/6$ state shown in Fig. 7(d) has a subharmonic at 1 GHz which doubles the period of the oscillation cycle. Note that as the repetition frequency of the injection pulses becomes higher, the behavior of the

Fig. 9. Regions of frequency-locked states of different ξ_p and f_{rep}. The shaded areas are the non-frequency locked regions (CO and CP).

To investigate the relation between each of these frequency-locked states, Fig. 8(a) plots the order of harmonics of f_{rep} (opened circle) and f_o (closed circle) for the frequency-locked states observed. In the low-repetition frequency regime, the order of f_o exceeds the order of f_{rep}. As can be seen, when f_{rep} exceeds about 3 GHz, the order of f_{rep} exceeds the order

of f_o. Orders as high as 8 for f_{rep} and 5 for f_o are obtained in our study. For frequency-locked states with even higher orders, the ranges of locking become very narrow. While the orders of f_{rep} and f_o do not show a clear trend, their ratio (winding number ρ) reveals the relation between each of the neighboring state.

Figure 8(b) plots the winding number of the frequency-locked states found for different repetition frequencies, where the widths of the intervals represent the ranges of locking. As can be seen, the locking states show a Devil's staircase structure [28], [29] that ρ decreases monotonically as f_{rep} increases. A Farey tree containing the observed Farey fractions [26] is also plotted in the upper-right corner showing the relation between each state. For f_{rep} below the relaxation oscillation frequency of the laser, $\rho = n + p/q$ with $n = 1$, 2, and 3 are found. For f_{rep} above the relaxation oscillation frequency, frequency-locked states with pure Farey fractions ($n = 0$) are obtained.

Note that while frequency-locked states with various orders are widely found in the weak injection condition considered ($\xi_p = 0.02$), finding frequency-locked states with higher order become difficult when the injection is stronger. Figure 9 shows the regions occupied by the frequency-locked states of different ρ with different ξ_p and f_{rep} for stronger injection (up to $\xi_p = 0.30$). As can be seen, with stronger injection, the laser tends to lock directly with the injected pulses so that the locking states of $\rho = 1/1$ ($f_o = f_{rep}$) dominate. High-order frequency-locked states are hardly seen when $\xi_p > 0.1$.

IV. CONCLUSION

We have numerically studied the nonlinear dynamics of a semiconductor laser under repetitive optical pulse injection. With the injection of a train of repetitive optical pulses, a semiconductor laser exhibits complex dynamics and it follows a period-doubling route to chaos. Both CO states and CP states are found, among which the CP states have broader bandwidths. Bandwidths as high as 14 GHz have been obtained for the CP states with $\xi_p = 0.30$. By varying the repetition frequency of the injected pulses, frequency-locked states with different winding numbers have also been investigated. The winding numbers reveal a Devil's staircase structure and the Farey tree constructed by the Farey fractions shows the relation between each neighboring frequency-locked state. For a wide range of repetition frequency spanning from 1 to 7 GHz, the oscillation frequencies of the frequency-locked states are found to be remained bounded close to the relaxation oscillation frequency of the laser. In the strong injection region, the laser tends to synchronize with the injected pulses and the frequency-locked states of $\rho = 1/1$ dominate. For the states found in this pulse injected laser, the chaos states can be used in applications demanding broad bandwidths such as ultra wideband communications and precise range finding, while the periodic oscillation states and the frequency locking states can be used in applications such as clock generation and recovery, wavelength conversion, and frequency stabilization.

REFERENCES

[1] F. Y. Lin and J. M. Liu, "Chaotic radar using nonlinear laser dynamics," IEEE J. of Quantum Electron. **40**, 815–820 (2004).
[2] F. Y. Lin and J. M. Liu, "Chaotic lidar," IEEE J. of Selected Topics in Quantum Electron. **10**, 991–997 (2004).
[3] R. Diaz, S. C. Chan, and J. M. Liu, "Lidar detection using a dual-frequency source," Opt. Lett. **31**, 3600-3602 (2006).
[4] S. C. Chan, S, K. Hwang, and J. M. Liu, "Radio-over-fiber AM-to-FM upconversion using an optically injected semiconductor laser," Opt. Lett. **31**, 2254-2256 (2006).
[5] C. R. Mirasso, P. Colet, and P. Garcia-Fernandez, "Synchronization of chaotic semiconductor lasers: Application to encoded communications," IEEE Photonics Technol. Lett. **8**, 299-301 (1996).
[6] I. Fischer, Y. Liu, and P. Davis, "Synchronization of chaotic semiconductor laser dynamics on subnanosecond time scales and its potential for chaos communication," Phys. Rev. A **62**, 011801 (2000).
[7] A. Argyris, D. Syvridis, L. Larger, V. Annovazzi-Lodi, P. Colet, I. Fischer, J. Garcia-Ojalvo, C. R. Mirrasso, L. Pesquera, and K. A. Shore, "Chaos-based communications at high bit rates using commercial fibre-optic links," Nature **438**, 343-346 (2005).
[8] F. Y. Lin and M. C. Tsai, "Chaotic communication in radio-over-fiber transmission based on optoelectronic feedback semiconductor lasers," Optics Express **15**, 302–311 (2007).
[9] J. Wang, M. K. Haldar, L. Li, and FVC Mendis, "Enhancement of modulation bandwidth of laser diodes by injection locking," IEEE Photonics Technol. Lett. **8**, 34–36 (1996).
[10] X. J. Meng, T. Chau, and M. C. Wu, "Experimental demonstration of modulation bandwidth enhancement in distributed feedback lasers with external light injection," Electron. Lett. **34**, 2031–2032 (1998).
[11] A. Takada and W. Imajuku, "Linewidth narrowing and optical phase control of mode-locked semiconductor ring laser employing optical injection locking," IEEE Photonics Technol. Lett. **9**, 1328-1330 (1997).
[12] F. Mogensen, H. Olesen, and G. X. Jacobsen, "FM noise suppression and linewidth reduction in an injection-locked semicondcutor-laser," Electron. Lett. **21**, 696–697 (1985).
[13] K. Inoue and K. Oda, "Noise suppression in wavelength conversion using a light-injected laser-diode," IEEE Photonics Technol. Lett. **7**, 500-501 (1995).
[14] S. Eriksson and A. M. Lindberg, "Periodic oscillation within the chaotic region in a semiconductor laser subjected to external optical injection," Opt. Lett. **26**, 142-144 (2001).
[15] T. B. Simpson, "Mapping the nonlinear dynamics of a distributed feedback semiconductor laser subject to external optical injection," Opt. Commun. **215,** 135–151 (2003).
[16] T. B. Simpson, J. M. Liu, A. Gavrielides, V. Kovanis, and P. M. Alsing,"Period-doubling route to chaos in a semiconductor-laser subject to optical-injection," Appl. Phys. Lett. **64**, 3539-3541 (1994).
[17] B. Krauskopf, S. Wieczorek, and D. Lenstra,"Different types of chaos in an optically injected semiconductor laser," Appl. Phys. Lett. **77**, 1611-1613 (2000).
[18] S. Wieczorek, B. Krauskopf, T. B. Simpson, and D. Lenstra,"The dynamical complexity of optically injected semiconductor lasers," Phys. Reports **416**, 1-128 (2005).
[19] A. Uchida, T. Heil, Y. Liu, P. Davis, and T. Aida, "High-frequency broad-band signal generation using a semiconductor laser with a chaotic optical injection," IEEE J. of Quantum Electron. **39**, 1462 (2003).
[20] Y. J. Wen, H. F. Liu, and D. Novak, "Optical signal generation at millimeter-wave repetition rate using semiconductor lasers with pulsed subharmonic optical injection," IEEE J. Quantum Electron. **37**, 1183-1193 (2001).
[21] Y. P. Zhao, Y. C. Wang, M. J. Zhang, Y. An, and J. L. Wang, "Period doubling in a Fabry-Perot laser diode subject to optical pulse injection," Chinese Phys. Lett. **24**, 1949-1952 (2007).
[22] J. Kaiser, I. Fischer, and W. Elsasser, "Mode locking of lateral modes in broad-area semiconductor lasers by subharmonic optical pulse injection," Appl. Phys. Lett. **88**, Art. No. 101110 (2006).
[23] F. Y. Lin and J. M. Liu, "Diverse waveform generation using semiconductor lasers for radar and microwave applications," IEEE J. of Quantum Electron. **40**, 682–689 (2004).

[24] J. M. Liu and T. B. Simpson, "Four-wave mixing and optical modulation in a semiconductor laser," IEEE J. of Quantum Electron. **30,** 957–965 (1994).
[25] H. G. Winful, Y. C. Chen, and J. M. Liu, "Frequency locking, quasiperiodicity, and chaos in modulated self-pulsing semiconductor lasers," Appl. Phys. Lett. **48,** 616-618 (1986).
[26] D. Baums, W. Elsässer, and E. O. Göbel, "Farey tree and devil's staircase of a modulated external-cavity semiconductor laser," Phys. Rev. Lett. **63**, 155-158 (1989).
[27] F. Y. Lin and J. M. Liu, "Harmonic frequency locking in a semiconductor laser with delayed negative optoelectronic feedback," Appl. Phys. Lett. **81**, 3128-3120 (2002).
[28] T. Gilbert and R. Gammon, "Stable oscillations and Devil's staircase in the Van der Pol oscillator," Int. J. of Bifurcation and Chaos **10**, 155-164 (2000).
[29] M. Jensen, P. Bak, and T. Bohr, "Complete Devils staircase, fractal dimension, and universality of mode-locking structure in the circle map," Phys. Rev. Lett. **50**, 1637-1639 (1983).

Shu-Ming Chang Shu-Ming Chang received the Ph.D. degree in Mathematics from National Tsing Hua University, Taiwan, in 2003. At present, he is an assistant professor with the Department of Applied Mathematics, National Chiao Tung University, Hsinchu, Taiwan. His research interests include numerical analysis and scientific computation.
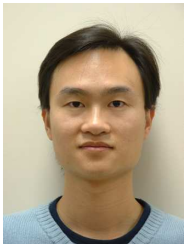
Fan-Yi Lin Fan-Yi Lin was born in Hsinchu, Taiwan. He received the B.S. degree in Electrophysics from National Chiao Tung University, Taiwan, in 1997 and the M.S. and Ph.D. degrees in Electrical Engineering from the University of California, Los Angeles, in 2001 and 2004, respectively.

He is currently an assistant professor with the Department of Electrical Engineering and Institute of Photonics Technologies, National Tsing Hua University, Hsinchu, Taiwan. His current research interests include nonlinear laser dynamics, optoelectronics, and lidar and radar systems.

Shiou-Yuan Tu Shiou-Yuan Tu was born in Taipei, Taiwan. He received the B.S. degree in Physics from National Changhua University of Education, Taiwan, in 2005 and the M.S. degree in Institute of Photonics Technologies from National Tsing Hua University, Taiwan, in 2007. His research interests include semiconductor lasers and communication systems.

Chien-Chih Huang Chien-Chih Huang was born in Taipei, Taiwan. He received the B.S. degree in Mathematics from Tamkang University, Taiwan, in 1998 and the M.S. degree in Mathematics from National Tsing Hua University, Taiwan, in 2000. At present, he is a Ph.D. student with the Department of Mathematics, National Tsing Hua University, Hsinchu, Taiwan. His research interests include chaotic dynamical systems and chaotic cryptosystems.